

Analytic Calculation of Shielding Effect of Vehicular Body on Low Frequency Magnetic Fields Induced by High Voltage Cables

Anika Henke, Robert Nowak, Stephan Frei

TU Dortmund University
Dortmund, Germany
anika.henke@tu-dortmund.de

Abstract—The electric propulsion system of modern electric vehicles may generate high magnetic fields in the low frequency range exceeding the thresholds for health protection. Mainly the currents through the three-phase cable system between the inverter and the electric motor are critical. This paper presents an analytic 2D solution for the magnetic fields from an infinite parallel cable system above an infinite plate. The solution considers the permeability, conductivity and thickness of the material. It is based on a fundamental solution of the diffusion equation and a Fourier-series development of the exciting line currents. The presented approach is fast and accurate for investigating the behavior of different cable arrangements and shielding materials. In this paper the shielding effect of vehicular bodies with different electrical properties is investigated. Several methods to reduce the resulting magnetic field are discussed.

Keywords—magnetic shielding; electric vehicles; analytic solution of diffusion equation

I. INTRODUCTION

Automobiles with electric drivetrain (EV) usually use three-phase machines with high currents. Critical low-frequency magnetic fields may appear as outlined in Fig. 1. To minimize interactions with the environment and persons, these fields have to comply given limits, e.g. [1]. The car body can be used as shield in order to reduce the fields in the passenger compartment, when cables are routed outside. The shielding properties of the car body have to be analyzed.

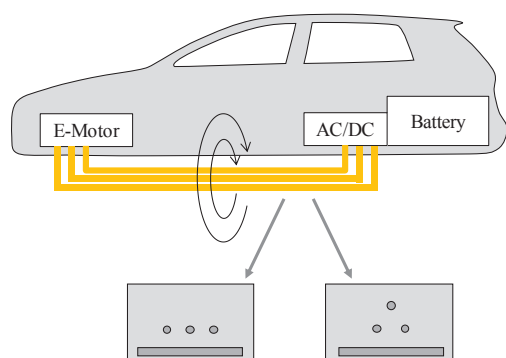


Fig. 1. Possible structure of an electric drivetrain with cables outside of the car body.

The consideration of a real car body as shield is complicated. Only for an infinite plane as shielding structure, some analytical solutions are given in the literature. In [2] a coil is used as excitation and in [3] two lines carrying a differential mode current are considered. Estimations for the shielding effect of metallic structures are given in [4]. Numerical approaches to compute the shielding efficiency are more flexible, but may have long computation times. In addition, the basic influence of the material and geometry parameters is hard to understand. Due to this reason an analytical 2D solution is presented here to describe the magnetic field of a cable system shielded by an infinite plane, assumed as approximation to the car body. It is assumed that the current carrying conductors are located under the car body outside the passenger compartment. To reduce the complexity of the approach the body is assumed as an infinite plate with known thickness, permeability and conductivity.

Mainly shielded cables are used for EV, but only the remaining leakage currents of the cables have to be considered, i.e. the cable system can be represented with filamentous conductors of infinite length. Below several hundred Hz the induced shielding currents are nearly zero and shielding efficiency of cable shield can be neglected anyway [5]. The EV-drive trains are driven by sinusoidal currents up to approx. 300 kHz and at low motor operation frequencies, the cable shield has no influence. With these assumptions, the partial differential equation for the magnetic vector potential can be solved using a Fourier series approach.

Different positions of the conductors as well as varying materials of the vehicular body are considered. The calculated magnetic flux densities are compared to the limits for human health protection and possible actions for compensation are discussed.

II. DETERMINATION OF THE ANALYTICAL SOLUTION

It is assumed that the magnetic as well as the electric properties of the shielding material are linear, homogenous and isotropic. Using the infinite extent of the structure, the resulting magnetic fields have no component parallel to the conductors, so there is no z -component. That is why this component is not noted in the following. Firstly, a “free” solution for the magnetic field without shield is presented, i.e. without any vehicular body. The magnetic flux density of a long conductor, parallel to the z -axis and flowing the current I , in the vacuum is given as

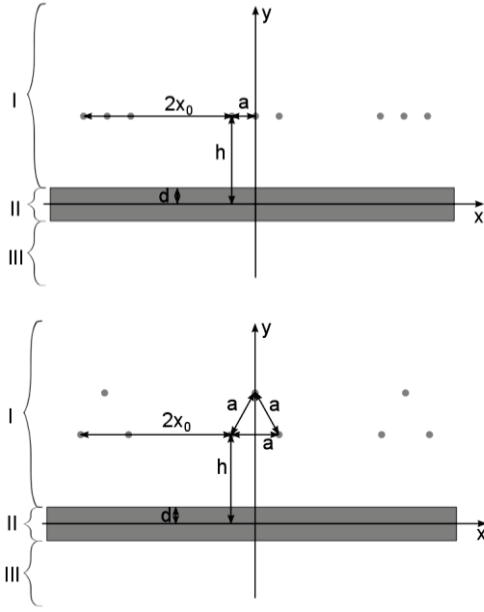


Fig. 2. Sketches of the studied configurations for the linear cable arrangement (top) and for the triangle cable arrangement (bottom).

$$\mathbf{B}(\mathbf{r}) = \frac{\mu_0 I}{2\pi r} \mathbf{e}_\varphi = \frac{\mu_0 I}{2\pi r^2} \begin{pmatrix} -r_y \\ r_x \end{pmatrix}. \quad (1)$$

Especially two different positions are examined, which are shown in Fig. 2. They are named “linear cable arrangement” and “triangle cable arrangement”. The free solution for a three-line system with a phase offset of 120° in the linear arrangement is:

$$\mathbf{B}_{\text{fr,linear}}(\mathbf{r}) = \frac{\mu_0 I}{2\pi} \left(\frac{e^{-\frac{j2\pi}{3}}}{(x+a)^2+(y-h)^2} \begin{pmatrix} -(y-h) \\ x+a \end{pmatrix} + \frac{1}{x^2+(y-h)^2} \begin{pmatrix} -(y-h) \\ x \end{pmatrix} + \frac{e^{\frac{j2\pi}{3}}}{(x-a)^2+(y-h)^2} \begin{pmatrix} -(y-h) \\ x-a \end{pmatrix} \right). \quad (2)$$

For the triangle cable arrangement, a similar solution can be found. Next, the solution considering the influence of an infinite plate with finite thickness as approximation for the vehicular body is presented. This is done in a similar approach like [3]. Like shown in Fig. 2, the computational area is split in three parts: the area I above the plate, the area II in the plate and the area III below the plate. In the following, \mathbf{A} names the magnetic vector potential, μ the permeability and σ the conductivity. The differential equation

$$\Delta \mathbf{A} = j\omega\mu\sigma \mathbf{A} \quad (3)$$

has to be solved, which is simplified in the areas I and II to the Laplace equation because of the vacuum conductivity of zero.

$$\Delta \mathbf{A} = 0 \quad (4)$$

First, the stimulation of the field is assumed to be periodically. Later the distance between the periodic repetitions will be

chosen wide enough so that the current (respectively the magnetic field) of the repetitions has a negligible effect. The current density of a single conductor is developed as one-dimensional Fourier series, depending on the x -coordinate.

$$\begin{aligned} f(x) &= \frac{I}{x_0} e^{j\varphi_1} \left(\frac{1}{2} + \sum_{n=1}^{\infty} \cos\left(\frac{n\pi}{x_0} x\right) \right) \\ &= \lim_{N \rightarrow \infty} \frac{I}{x_0} e^{j\varphi_1} \sum_{n=1}^N \left(\frac{1}{2N} + \cos\left(\frac{n\pi}{x_0} x\right) \right) \end{aligned} \quad (5)$$

The magnetic vector potential is modeled by a separation of variables: The x -dependence is chosen like the stimulation, for the y -dependence initially unknown functions F_{In} , F_{IIIn} and F_{IIIIn} are assumed. This approach is inserted into the differential equations (3) and (4). It results new differential equations for the y -dependence:

$$\left(\frac{n\pi}{x_0}\right)^2 \cdot F_{\text{In}}(y) = \frac{\partial^2}{\partial y^2} F_{\text{In}}(y), \quad (6)$$

$$\left(\alpha^2 + \left(\frac{n\pi}{x_0}\right)^2\right) \cdot F_{\text{IIIn}}(y) = \frac{\partial^2}{\partial y^2} F_{\text{IIIn}}(y), \quad (7)$$

$$\left(\frac{n\pi}{x_0}\right)^2 \cdot F_{\text{IIIIn}}(y) = \frac{\partial^2}{\partial y^2} F_{\text{IIIIn}}(y). \quad (8)$$

Here it applies $\alpha^2 = j\omega\sigma\mu$. These differential equations are solved with function approaches, which consider the geometry:

$$F_{\text{In}}(y) = C_{\text{In}} \cdot e^{-\frac{n\pi}{x_0}|y-h|} + D_{\text{In}} \cdot e^{\frac{n\pi}{x_0}y}, \quad (9)$$

$$F_{\text{IIIn}}(y) = C_{\text{IIIn}} \cdot e^{k_n(y+d)} + D_{\text{IIIn}} \cdot e^{-k_n(y+d)}, \quad (10)$$

$$F_{\text{IIIIn}}(y) = C_{\text{IIIIn}} \cdot e^{\frac{n\pi}{x_0}y} \quad (11)$$

with $k_n = \sqrt{\alpha^2 + \left(\frac{n\pi}{x_0}\right)^2}$. To determine the parameters C_{In} and D_{In} , Ampère's law and the transition conditions between the different areas are applied. Thus, an equation system is given having the solutions:

$$C_{\text{In}} = \frac{\mu_0 x_0}{2n\pi}, \quad (12)$$

$$D_{\text{In}} = \frac{C_{\text{In}}}{N_n} \left(\beta_n - \frac{1}{\beta_n} \right) e^{\frac{n\pi}{x_0}(2d-h)} \sinh(2k_n d), \quad (13)$$

$$C_{\text{IIIn}} = \frac{C_{\text{In}}}{N_n} (1 + \beta_n) e^{\frac{n\pi}{x_0}(d-h)}, \quad (14)$$

$$D_{\text{IIIn}} = \frac{C_{\text{In}}}{N_n} (1 - \beta_n) e^{\frac{n\pi}{x_0}(d-h)}, \quad (15)$$

$$C_{\text{IIIIn}} = 2 \frac{C_{\text{In}}}{N_n} e^{\frac{n\pi}{x_0}(2d-h)} \quad (16)$$

with

$$\beta_n = \frac{\mu_r n \pi}{x_0 k_n}, \quad (17)$$

$$N_n = \left(\beta_n + \frac{1}{\beta_n} \right) \sinh(2k_n d) + 2 \cosh(2k_n d). \quad (18)$$

Finally, the solutions for the magnetic vector potential in the different areas are given:

$$A_I = \lim_{N \rightarrow \infty} \sum_{n=1}^N F_{In}(y) \frac{I}{x_0} e^{j\varphi_1} \left(\frac{1}{2N} + \cos\left(\frac{n\pi}{x_0} x\right) \right), \quad (19)$$

$$A_{II} = \lim_{N \rightarrow \infty} \sum_{n=1}^N F_{II n}(y) \frac{I}{x_0} e^{j\varphi_1} \left(\frac{1}{2N} + \cos\left(\frac{n\pi}{x_0} x\right) \right), \quad (20)$$

$$A_{III} = \lim_{N \rightarrow \infty} \sum_{n=1}^N F_{III n}(y) \frac{I}{x_0} e^{j\varphi_1} \left(\frac{1}{2N} + \cos\left(\frac{n\pi}{x_0} x\right) \right). \quad (21)$$

This is the solutions for a single conductor. The solution for several conductors is the superposition of these solutions. The magnetic flux density can be calculated by using the rotation operator on the magnetic vector potential:

$$B_{ix} = \frac{\partial A_i}{\partial y}, \quad B_{iy} = -\frac{\partial A_i}{\partial x}. \quad (22)$$

In the special case of three equidistant conductors in the height h above the vehicular body, the Fourier series of the stimulation is calculated at once. Thus, a solution for the magnetic vector potential results without any superposition. In this case computation time can be reduced.

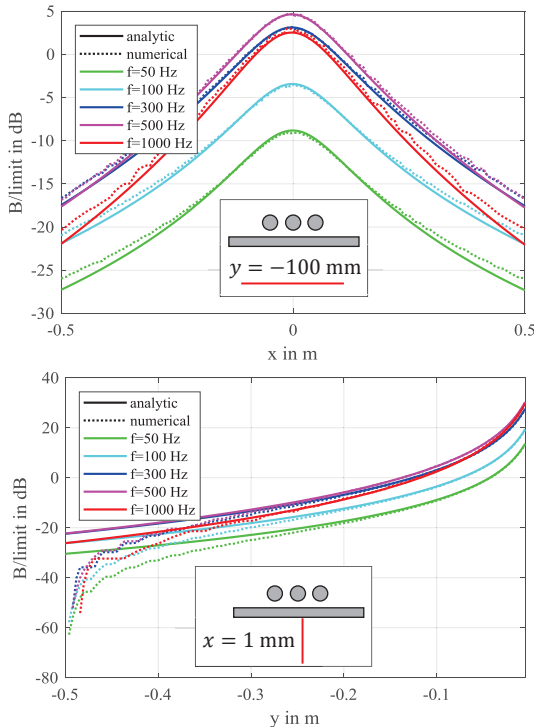


Fig. 3. Scaled magnetic flux density in dB for different frequencies along the given contours, calculated using the analytic and the numerical solution.

TABLE I
GEOMETRY PARAMETERS AND VALUES OF INVESTIGATED
LINEAR CABLE CONFIGURATION

Parameter	Value	Description
d	0.4 mm	half width of the plate thickness
I	400 A	amplitude of the current through the conductors
x_0	10 m	half distance between the periodic repetitions
f	300 Hz	frequency of the stimulating currents
a	11 mm	distance between the different conductors (diameter of the conductors)
h	$d + 1 \text{ mm} + \frac{a}{2}$ $= 6.9 \text{ mm}$	height of the conductors above the x -axis, assuming an isolation (thickness 1 mm)
N	20 000	maximal index

TABLE II
ICNIRP LIMITS FOR PERSONS [1]

Frequency f in Hz	Limit in μT
50	100
100	50
300	16.67
500	10
1000	6.25

TABLE III
PARAMETERS OF INVESTIGATED MATERIALS

Material	μ_r	σ in S/m
steel [7]	500	$5.88 \cdot 10^6$
aluminum [8]	1	$3.96 \cdot 10^7$
iron ₁ [8]	5000	$10.3 \cdot 10^6$
iron ₂	500	$10.3 \cdot 10^6$

In [3] the solution for a pair of two cables is presented. It is also possible to generate a solution for a single conductor by using this result. In this case, the distance between the two conductors has to be chosen wide enough to neglect the influence of the second conductor.

III. VALIDATION WITH NUMERICAL SOLUTION

To verify the presented approach, the magnetic fields of an exemplary cable system assumed to be used in an EV are calculated. In Table I, typical parameter values are shown. These values are also used in the following if not stated differently. The analytic solution is compared with a numerical solution of (3), which is calculated with the PDE Toolbox of MATLAB [6]. In the numerical solution, the conductor radius is set to 1 mm and the shield is neglected. Fig. 3 shows the magnetic flux density on the contours $y = -100 \text{ mm}$ and $x = 1 \text{ mm}$ for various frequencies of both approaches. The magnetic flux density is related to the limits for persons. Here, the limit published by ICNIRP in 1998 are used [1]. Later, higher limits were published by ICNIRP. Nevertheless, in this consideration, the previous limits are used, as those are stricter and still in use today. The comparison of the solutions shows a good match, only due to the discretization of the numerical approach some deviations can be observed. For several frequencies used in the following, the limits of [1] are shown in Table II. In Table III, the characteristic parameters of the later used materials are presented. If not stated differently, steel is considered.

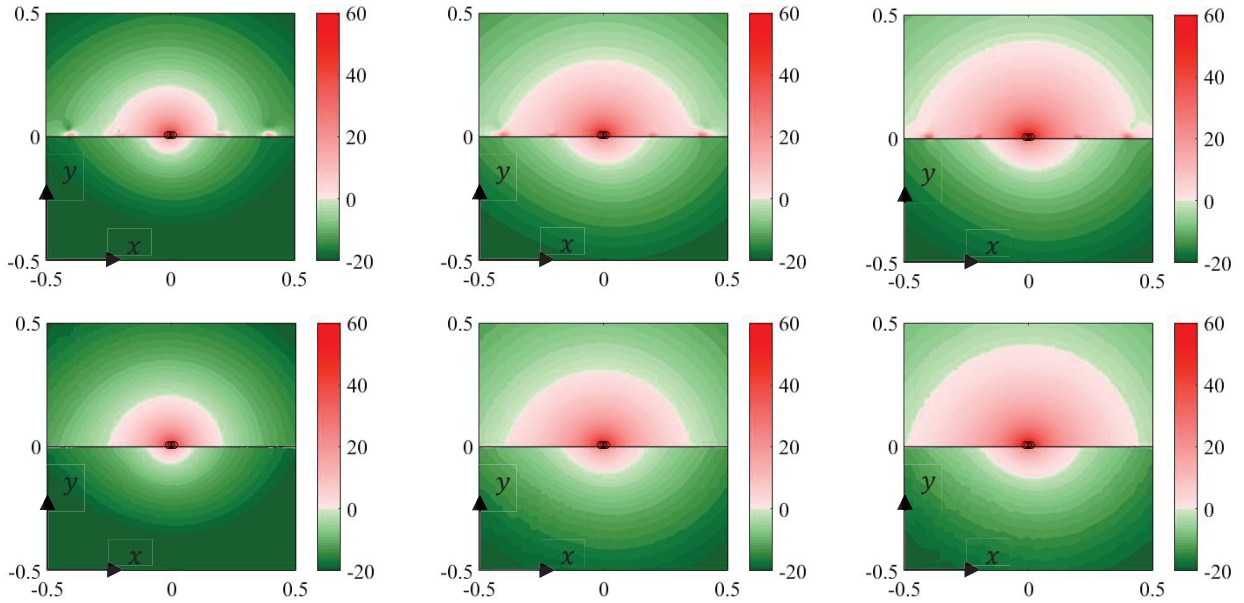


Fig. 4. Resulting magnetic flux density scaled with the limit in dB for different frequencies (left: 100 Hz, middle: 300 Hz, right: 500 Hz) calculated with the analytic solution (top) and the numerical solution (bottom). x and y for each plot in m.

IV. MAGNETIC FIELDS OF A HV-AC-SYSTEM AND COMPARISON TO THE LIMIT VALUES FOR PERSONS

In electric vehicles, normally the two arrangements shown in Fig. 2 are of potential interest. Here, we focus on the so-called linear cable arrangement. For different frequencies of the stimulating currents, different magnetic flux densities result. Those are exemplarily shown in Fig. 4. Depending on the x - and y -coordinates in meters, the ratio between the induced magnetic

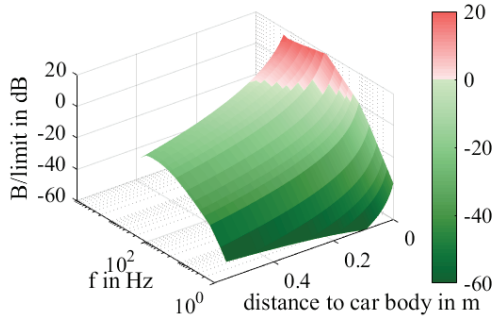


Fig. 5. Magnetic flux density related to the limits in dB for various frequencies and distance to the body.

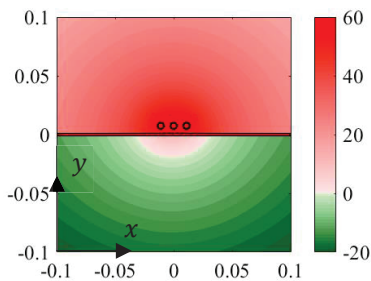


Fig. 6. Magnetic flux density related to the limits in dB for a thickness of 2 mm of the vehicular body.

flux density and its limit for persons in dB is presented, calculated with the analytic solution (upper plots) as well as with the numerical solution (lower plots). In the numerical PDE-model, the conductor system is stimulated with voltages sources. Here, the source voltages are adjusted to (radius 3.33 mm) impress a current of about 400 A. Every conductor has a massive shield made of copper (shield radius 4.9 mm, thickness 0.3 mm, conductivity $56 \cdot 10^6$ S/m). The simulated leakage current is used as stimulating current sources in the analytical solution. As expected, both solutions give similar results. The numerical solution is not as smooth as the analytical solution in higher distances from the conductors because of the coarse triangular discretization. Overall, in this comparison it is shown that the analytic solution is viable to investigate the exceeding of the magnetic flux density limit.

Neglecting the shields of the conductors, the exceedance of the limit is investigated for the linear cable arrangement described in Table I. The dependency from the frequency is presented in Fig. 5. Here the magnetic flux related to the limits along the vertical centric contour below the body is shown. The highest exceedance from the threshold can be observed at about 300 Hz. In the following, for this frequency, the effect of different actions for reduction of the limit exceeding is investigated.

V. ACTIONS FOR REDUCTION OF LOCAL FIELDS

To reduce the magnetic fields, different approaches are possible. Firstly, a variation of geometry and material parameters is examined. Afterward, the usage of compensation currents is discussed. All investigations in this chapter are done for a stimulus at 300 Hz.

A. Geometry and Material Parameters of Vehicular Body

By increasing the material thickness, the shielding efficiency increases. In Fig. 6, the normalized magnetic flux density for a steel sheet of 2 mm thickness is shown. Compared to the flux

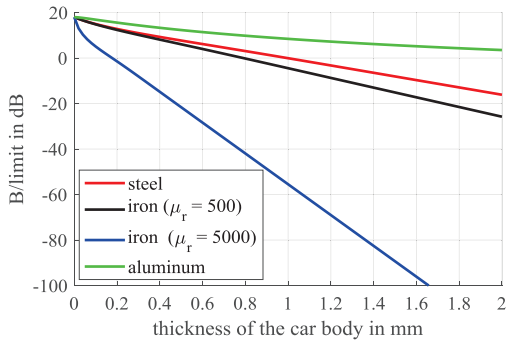


Fig. 7. Magnetic flux density scaled with the limits in dB for different materials and $(x|y) = (0 \text{ cm}| -10 \text{ cm})$.

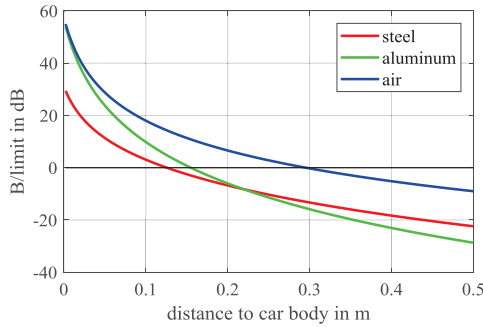


Fig. 8. Normalized magnetic flux density in dB for a thickness of the car body of 0.8 mm .

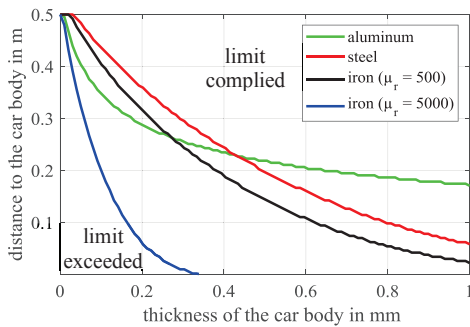


Fig. 9. Combinations for the thickness of the car body and the distance to the car body for meeting the threshold for different materials

distribution in Fig. 5 (middle), an improvement can be seen. Below the sheet, the emission limit nearly everywhere can be met.

The effect of different materials is shown in Fig. 7. Here, the magnetic flux density 10 cm below the center of the body in the middle of the configuration ($x = 0 \text{ cm}$) related to the limits is shown over the plane thickness. With rising thickness, the magnetic flux density decreases. Materials with high relative permeability provide better performance, as expected.

In Fig. 8, the magnetic flux density below the body along a vertical contour (centric in the configuration) for different materials is presented. Comparing the flux density for steel or aluminum with the flux density for air, the shielding efficiency for both materials is shown.

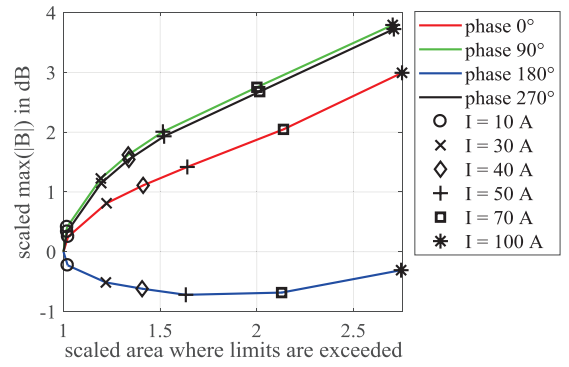


Fig. 10. Relation between the maximum magnetic flux density and the area where limits are exceeded, normalized to the case without compensation.

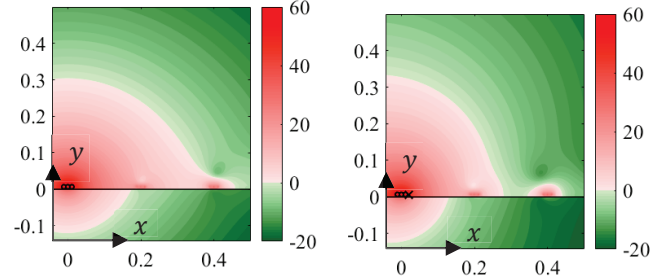


Fig. 11. Resulting magnetic flux density without compensation (left) and with compensation (right).

The examinations of Fig. 7 and Fig. 8 are merged in Fig. 9. Here, for different materials, boundaries are shown which represent the necessary thickness of the car body to comply with the limit in a given distance to the body. Like in Fig. 7, the supporting effect of high permeable materials is outlined.

B. Actions for Compensations

Another approach to comply the limits is the usage of a compensating current in an additional conductor or set of conductors. Therefore, another conductor can be added to the system or a current can be injected in the shields if shielded cables are used. Injecting an inverse current in each shield means full compensation of the resulting fields. However, this approach is not reasonable because of the necessary thickness of the shields to carry the inverse current.

One approach to reduce the fields is the injection of a current in another external conductor with varying current strength and phase. The relation between the area with exceeded limits and the maximum magnetic flux density related to the case without any compensation for different phases of the compensations current is shown in Fig. 10. Here, the configuration of Table I with a compensation conductor 6.6 mm above the original conductor configuration is examined. At first, a greater influence on the phase of the compensation current as current strength can be recognized. For a higher compensating current, the area with exceeded limits generally increases. A slightly decrease as well as a huge increase of the maximal magnetic flux density is possible. This is why an improvement for a concrete use can be achieved, especially if there is only a small exceedance of the limits.

The most important question related to an external compensation conductor is the reduction of the magnetic field in critical volumes. An exemplary case is shown in Fig. 11. In addition to the linear cable arrangement (Table I), a compensating current of $30 \text{ A} \cdot e^{j3\pi/2}$ is placed 1 cm to the right of the cable configuration at the same height. Here, the magnetic flux density decreases at $x \approx 0.3 \text{ m}$ in comparison to the case without compensation. A local improvement can be achieved. The center point of this area can be controlled with the location of the compensation conductor.

VI. SUMMARY

In this paper, an analytic approach for the calculation of the magnetic field of a cable system above a metallic ground plane as a substitute for a vehicular car body is presented. This solution is faster and more accurate than numerical solutions. It is used to investigate the shielding efficiency of different materials. An appropriate material and material thickness can be found in order to comply with health protection limits. Furthermore, the analytic solution is also used for discussing the effect of compensating conductors. The flux densities can be reduced in this way for critical areas.

REFERENCES

- [1] International Commission on Non-Ionizing Radiation Protection: "ICNIRP Guidelines for Limiting Exposure to Time-Varying Electric, Magnetic and Electromagnetic Fields (up to 300 GHz)," *Health Physics*, vol. 74, no. 4, pp. 494 – 522, Apr. 1998.
- [2] J. R. Moser, "Low-Frequency Shielding of a Circular Loop Electromagnetic Field Source," *IEEE Trans. Electromagn. Compat.*, vol. 9, no. 1, pp. 6 – 18, Mar. 1968.
- [3] A. Kost and M. Ehrlich, "Abschirmung magnetischer Störfelder mit Stahlplatten," in *3. Internat. Kongress f. Elektromagnetische Verträglichkeit*, Karlsruhe, Germany, Feb. 1992, pp. 421 – 432.
- [4] M. Kühn, W. John, and R. Weige, "Validation of a measurement method for magnetic shielding effectiveness of a wire mesh enclosure with comparison to an analytical model," *Adv. Radio Sci.*, vol. 11, pp. 189 – 195, Jul. 2013.
- [5] S. Frei, A. Mushtaq, K. Hermes, and R. Nowak, "Current Distribution in Shielded Cable-Connector Systems for Power Transmission in Electric Vehicles," in *Proc. Asia-Pacific Int. Symp. Electromagn. Compat.*, Singapore, May 2018.
- [6] *Partial Differential Equation Toolbox™. User's Guide. R2016b*, The MathWorks Inc., Natick, MA, 2016.
- [7] M. Klingler, "Modeling and simulation of powertrains for electric and hybrid vehicles," presented at *2009 IEEE Int. EMC Symp.*, Austin, TX, USA, 2009. [Online], Available: http://www.jastech-emc.com/papers/IEEE-EMC_TP4_2009.pdf [Accessed May 14, 2018].
- [8] F. M. Tesche, M. Ianoz and T. Karlsson, *EMC Analysis Methods and Computational Models*, New York, NY, USA: Wiley, 1997.